Evolution and Functional Diversification of Fructose Bisphosphate Aldolase Genes in Photosynthetic Marine Diatoms

Andrew E. Allen,[1,2] Ahmed Moustafa,†[,2] Anton Montsant,[1,3] Angelika Eckert,[4] Peter G. Kroth,[4] and Chris Bowler*[,1,3]

[1]Environmental and Evolutionary Genomics Section, Institut de Biologie de l'Ecole Normale Supéreure, CNRS UMR8186 INSERM U1024, Ecole Normale Supérieure, Paris, France

[2]Microbial and Environmental Genomics, J. Craig Venter Institute, San Diego, California

[3]Laboratory of Cell Signaling, Stazione Zoologica Anton Dohrn, Naples, Italy

[4]Plant Ecophysiology, Fachbereich Biologie, Universität Konstanz, Konstanz, Germany

†Present address: Department of Biology and Biotechnology Graduate Program, American University in Cairo, New Cairo, Egypt

***Corresponding author:** E-mail: cbowler@biologie.ens.fr.

Associate editor: Charles Delwiche

Research article

Abstract

Diatoms and other chlorophyll-*c* containing, or chromalveolate, algae are among the most productive and diverse phytoplankton in the ocean. Evolutionarily, chlorophyll-*c* algae are linked through common, although not necessarily monophyletic, acquisition of plastid endosymbionts of red as well as most likely green algal origin. There is also strong evidence for a relatively high level of lineage-specific bacterial gene acquisition within chromalveolates. Therefore, analyses of gene content and derivation in chromalveolate taxa have indicated particularly diverse origins of their overall gene repertoire. As a single group of functionally related enzymes spanning two distinct gene families, fructose 1,6-bisphosphate aldolases (FBAs) illustrate the influence on core biochemical pathways of specific evolutionary associations among diatoms and other chromalveolates with various plastid-bearing and bacterial endosymbionts. Protein localization and activity, gene expression, and phylogenetic analyses indicate that the pennate diatom *Phaeodactylum tricornutum* contains five FBA genes with very little overall functional overlap. Three *P. tricornutum* FBAs, one class I and two class II, are plastid localized, and each appears to have a distinct evolutionary origin as well as function. Class I plastid FBA appears to have been acquired by chromalveolates from a red algal endosymbiont, whereas one copy of class II plastid FBA is likely to have originated from an ancient green algal endosymbiont. The other copy appears to be the result of a chromalveolate-specific gene duplication. Plastid FBA I and chromalveolate-specific class II plastid FBA are localized in the pyrenoid region of the chloroplast where they are associated with β-carbonic anhydrase, which is known to play a significant role in regulation of the diatom carbon concentrating mechanism. The two pyrenoid-associated FBAs are distinguished by contrasting gene expression profiles under nutrient limiting compared with optimal CO_2 fixation conditions, suggestive of a distinct specialized function for each. Cytosolically localized FBAs in *P. tricornutum* likely play a role in glycolysis and cytoskeleton function and seem to have originated from the stramenopile host cell and from diatom-specific bacterial gene transfer, respectively.

Key words: carbon concentrating mechanism (CCM), carbon metabolism, carbonic anhydrase, diatom, fructose bisphosphate aldolase, pyrenoid.

Introduction

It is believed that the diatom lineage emerged less than 300 Ma. Considering the diversity of extant diatom species, comparable to that of angiosperms (Round et al. 1990), diatoms have displayed a remarkable diversification rate and plasticity for adaptation to new environments. Mechanisms for assimilation and recycling of major nutrients, such as carbon (C), nitrogen (N), phosphorus (P), or iron (Fe) likely present notable differences from those known in green algae and plants and may provide insights about the ability of diatoms to thrive and diversify in aquatic environments (Wilhelm et al. 2006; Armbrust 2009; Bowler et al. 2010). For example, diatoms possess a urea cycle, previously known only in metazoans, through which organic nitrogen may be recycled (Armbrust et al. 2004; Allen et al. 2006, 2011), and they may utilize siderophore-based iron uptake like in cyanobacteria (Allen et al. 2008).

Diatoms are responsible for up to 40% of annual primary productivity in the ocean (Field et al. 1998; Granum et al. 2005). Diatom RuBisCO (ribulose 1,5-bisphosphate carboxylase/oxygenase) enzymes, however, have half saturation constants for CO_2 of 30–60 μM (Badger et al. 1998), whereas seawater typically contains around 10 μM CO_2, which implies that marine diatoms would be CO_2-limited in the absence of a carbon concentrating mechanism (CCM) (Riebesell et al.

1993) (Hopkinson et al. 2011; Reinfelder 2011). The relatively high affinity of diatom cells for CO_2, coupled with the observation that diatom populations commonly reach bloom densities, indicates that diatoms possess efficient CCMs (Badger et al. 1998; Roberts et al. 2007a, 2007b; Bowler et al. 2010; Hopkinson et al. 2011; Reinfelder 2011).

In recent years, the CCMs, through which diatoms ensure the supply of CO_2 to RuBisCO, have attracted increasing attention (Roberts et al. 2007b). Green algae typically utilize bicarbonate transporters in combination with plastid, cytosol, and cell surface carbonic anhydrases (CAs), which catalyze conversion between CO_2 and bicarbonate, as a mechanism of promoting CO_2 supply to RuBisCO, much like the biophysical CCMs that have been reported in cyanobacteria (Kaplan and Reinhold 1999). Diatom genome sequences unambiguously indicate the presence of different HCO_3- transport systems (Kroth et al. 2008). In *Phaeodactylum tricornutum*, at least one such transporter has an N-terminal plastid-targeting precursor (Allen et al. 2008; Kroth et al. 2008). *Phaeodactylum tricorutum* is also known to contain a plastid-targeted β-carbonic anhydrase (β-CA) (Montsant et al. 2005; Kitao et al. 2008; Tachibana et al. 2011).

In diatoms, a putative C_4-like mechanism has also been proposed to explain their efficient C fixation under CO_2 and Zn limitation (Reinfelder et al. 2000, 2004; Reinfelder 2011). However, conflicting experimental data for support of C_4 photosynthesis in diatoms has been reported (Roberts et al. 2007a; McGinn and Morel 2008), and genomic data does not fully clarify the presence and localization of the enzymes that may drive this mechanism (Kroth et al. 2008; Parker et al. 2008; Bowler et al. 2010). It is possible that individual diatom species may rely to a different extent on both biophysical and biochemical CCMs in order to optimally regulate efficient inorganic carbon acquisition.

Potential links between diatom CCMs and other aspects of C metabolism such as the direction of C flow between C_3 and C_6 sugar pools and sustained regeneration of the C_5 RuBisCO substrate ribulose 1,5-bisphosphate (Ru 1,5-BP) have not been addressed. β-CA and putatively plastidic fructose 1,6-bisphosphate aldolase (FBA) are downregulated and upregulated, respectively, in iron-limited *P. tricornutum* cells (Allen et al. 2008), which are known to display compromised photosystem reaction centers, reduced photosynthetic electron transfer rates, decreased reductant production, and an inability to efficiently process absorbed photons (Behrenfeld et al. 1996, 2006; Milligan and Harrison 2000). This has prompted speculation that plastidic β-CA and FBA are part of a coordinated effort to regulate carbon flux within the plastid during periods of energy limitation (Allen et al. 2008). FBA genes have been noted for their peculiar phylogenetic distribution and highlighted in several comparative genomic studies (Kroth et al. 2005, 2008; Montsant et al. 2005) and due to important roles in balancing C_6 and C_3 sugar pools in the Calvin–Benson cycle and glycolysis, as likely key regulators for the flow of small organic C molecules and CO_2 in the plastid and cytosol. There are two evolutionarily unrelated FBAs, termed class I and class II, with a very complex phylogenetic distribution. These two types do not share sequence similarity with each other and their catalytic mechanism is different; unlike class I FBAs, class II FBAs are dependent on divalent cations and, therefore, constitute a case of convergent functional evolution (Marsh and Lebherz 1992).

Class I and class II FBAs catalyze the interconversion between C_3/C_4 molecules and C_6/C_7 molecules (Flechner et al. 1999). Therefore, FBAs can be involved both in carbon fixation and in glycolysis. In Calvin–Benson cycle reactions, the C_5 molecule ribulose 1,5-bisphosphate (Ru 1,5-BP) is carboxylated and split into C_3 molecules that are reduced to glyceraldehyde 3-phosphate (G3P). The formation of the hexose sugars glucose and fructose as well as regeneration of Ru 1,5-BP requires the action of FBA, which catalyzes the formation of the C_6 compound fructose 1,6-bisphosphate from two C_3 G3P molecules and dihydroxyacetone phosphate (DHAP). On the other hand, in glycolytic reactions FBAs split C_6 molecules into C_3 molecules, which are transformed into pyruvate. Pyruvate can then be transformed to acetyl coenzyme A and oxidized to CO_2 through the Krebs cycle in the mitochondria or enter biosynthetic pathways such as fatty acid or amino acid biosynthesis.

In animals, only class I FBAs are known, whereas fungi appear to rely solely on FBA II (Jacobshagen and Schnarrenberger 1990; Marsh and Lebherz 1992; Pelzer-reith et al. 1993) (table 1). Red algae and glaucocystophytes have been reported to have class II FBAs in their cytosol and class I FBA in their plastids, although the sampling of these eukaryotic lineages has been limited to date (Anita 1967; Gross et al. 1994, 1999). The two classes of FBA have been detected in Eubacteria (including Cyanobacteria), although these organisms most typically utilize class II FBAs (Sanchez et al. 2002). Although FBA I activity was detected in the diatom *P. tricornutum* in an early study (Anita 1967), secondary endosymbiotic algae, commonly referred to as Chromalveolata (Cavalier-Smith 2000), such as diatoms, dinoflagellates, haptophytes, and cryptophytes, which are believed to have inherited their plastids from red algae in a unifying single event (Yoon et al. 2002), are generally thought to utilize class II FBAs both in cytosol and in plastids (Anita 1967; Rogers and Keeling 2004). The universal occurrence of class II type A FBA in chromalveolate plastids coupled with an apparent lack of red alga-like plastid-targeted FBA I was previously interpreted as evidence for a chromalveolate-specific gene replacement that supports the single origin of chromalveolate plastids (Patron et al. 2004). More recently, statistical analyses of phylogenomic data have been used to argue for falsification of the single origin of Chromalveolata in favor of more complex evolutionary scenarios such as serial acquisition of secondary plastids by distantly related hosts (Baurain et al. 2010). Whether chromalveolate plastids evolved from a single endosymbiotic event or from serial transfer between diverse hosts, genomic data for key outgroups indicates an unambiguously common line of descent for Chromalveolata plastids (Janouskovec et al. 2010).

Although a single gene family such as Fba will not resolve the conflicts surrounding the origin of chromalveolate plastids,

Table 1. Distribution of FBA Genes in Eukaryotes.

Eukaryotic Lineage	Eukaryotic Crown Group	Plastid FBA	Cytosol FBA	References
Plants	Viridiplantae	I	I, IIB	Jacobshagen and Schnarrenberger (1990); Pelzer-Reith et al. (1993)
Red algae	Viridiplantae	I	I^a, II	Anita (1967); Kroth et al. (2005); This work
Glaucophytes	Viridiplantae	IIB	I^a, II	Gross et al. (1994); This work
Prasinophytes	Viridiplantae	I^a, II^a	I^a, (+ I^b)^a	This work
Oomycetes	Heterokonts	—	II	Kroth et al. (2005)
Diatoms[c]	Heterokonts	$(I^{py})^a$, II, $(II^{py})^a$	II, I^a, (+ I^b)	Patron et al. (2004); Kroth et al. (2005); Montsant et al. (2005)
Haptophyta	Chromalveolates[d]	$(I^{py})^a$, II^a, $(II^{py})^a$	I^a, II^a	This work
Cryptophytes	Chromalveolates[d]	I, $(II^{py})^a$	I^a	Patron et al. (2004); This work
Apicomplexa	Alveolates	—	I	Rogers and Keeling (2004)
Dinoflagellates	Alveolates	(I^{py}), $(II^{py})^a$	I^a, II^a	Kroth et al. (2005); This work
Chlorarachniophyte	Rhizaria	I	I, II^a	Rogers and Keeling (2004)
Animals	Opisthokonts	—	I	Marsh and Lebherz (1992)
Fungi	Opisthokonts	—	II	Marsh and Lebherz (1992)

NOTE.—The two known types of FBAs can participate in glycolytic reactions in the cytosol and in Calvin–Benson cycle reactions in the plastid. The two types are also widespread between Archaea and Eubacteria. ^{py} indicates plastidic FBAII or FBAI localized to the pyrenoid. Pyrenoid localization of FBA has only been confirmed in *P. tricornutum*.

[a] Denotes first report in this work.

[b] This cytosolic type-I FBA is a divergent, bacterial-derived variant dissimilar to type-I FBAs known in other eukaryotes.

[c] *Phaeodactylum tricornutum* has three putative plastid FBAs (the respective genes termed FBAC1, FBAC2, and FBAC5) and two cytosolic FBAs (FBA3 and FBA4). FBA4 and FBAC5 are type-I FBAs.

[d] Haptophya and Cryptophyta are closely related to Heterokonts and together with diatoms and brown algae (stramenopiles), and dinoflagellates (alveolates) are known as chromalveolates.

information related to the phylogenetic distribution and function of different FBA types will help to clarify the evolutionary and physiological significance of different FBAs within and among different algal groups. Preliminary comparative analyses of the distribution of *FBA* family genes in diatoms based on the genome sequence of the centric diatom *Thalassiosira pseudonana* and expressed sequence tag (EST) data from *P. tricornutum* revealed several surprising features (Montsant et al. 2005). On the one hand, diatoms appeared to be the only eukaryotes to possess a typically bacterial class I FBA, termed FBA4 (Kroth et al. 2005), for which no targeting sequence was detected (i.e., likely a cytosolic enzyme). Additionally, the pennate diatom *P. tricornutum* appeared to have a plastid-localized class I FBA, FBAC5 (Kroth et al. 2005; Montsant et al. 2005), which are usually found in the green and red algal lineages rather than in chromalveolate algae (Patron et al. 2004). This phylogenetic puzzle poses functional questions when considering that both *T. pseudonana* and *P. tricornutum* also have the class II plastid and cytosolic FBAs expected in chromist algae (Patron et al. 2004), denoted FBAC1, FBAC2, and FBA3 in *P. tricornutum* (Kroth et al. 2005). We have therefore characterized each *P. tricornutum* FBA phylogenetically, using genome sequence or EST data now available for each of the major lineages of eukaryotic photosynthetic algae. To generate further information about functionality, we have also examined their subcellular localization and evaluated gene expression under different conditions. We specifically evaluated FBA transcriptional responses to Fe limitation because previous studies based primarily on EST sequencing suggested that certain FBA genes are responsive to Fe availability (Allen et al. 2006; Maheswari et al. 2010). Iron availability is also known to heavily influence diatom physiology and metabolism (Kustka et al. 2007; Allen et al. 2008) and distribution (Behrenfeld et al. 2006).

Materials and Methods

Phaeodactylum tricornutum Cultures

Axenic cultures of *P. tricornutum* Bohlin clone CCMP2560 (Provasoli-Guillard National Center for Culture of Marine Phytoplankton, Bigelow) were grown in f/2 medium made with 0.2 μm filtered and autoclaved seawater supplemented with f/2 vitamins and inorganic nutrients (Guillard 1975). Cell cultures were grown to midexponential phase at a temperature of 18 °C and a 16:8 light (150 μE/m/sec):dark regime. Sterility was monitored by inoculation into peptone-enriched media to detect bacterial growth. For iron limitation experiments, Fe was precomplexed with EDTA (1:1.1 mol:mol) and added (5 nM Fe) to Fe-free media. Cells were cultured in semicontinuous mode until growth rates stabilized. Cultures were diluted with fresh medium at a rate of approximately 0.1–0.2 per day depending on growth rate and were maintained in a state of exponential growth. Fe′, the sum of all unchelated species, calculated according to equations of Sunda and Huntsman (2003) was ($Fe' = 0.0024\ Fe_T$) under our conditions. Therefore, the Fe-limiting condition had an Fe′ level of 12.0 pmol·liters^{-1} Fe′ and the Fe replete condition had an Fe′ value of 2.6 nmol·liters^{-1} Fe′.

The availability of free Fe ions in the culture media was effectively buffered to maintain consistent Fe′ levels over the course of the experiments. Growth rates were monitored by cell counting via microscopy before and after dilution. Generally, the growth rate of cells in iron-limited cultures was around 60% of the maximum growth rate in iron-replete cultures. Iron limitation was confirmed by following the recovery of high growth rate following addition of iron to a small volume of the culture.

Cloning of *P. tricornutum* Genes

The five *Fba* genes and a plastid-localized β-CA (*CA1*) described earlier (Tanaka et al. 2005) were cloned into Gateway

diatom expression vectors (Siaut et al. 2007). The primers and cDNA templates used for polymerase chain reaction (PCR) amplification are indicated in supplementary table S1 (Supplementary Material online). Correctly sized amplicons were cloned into Gateway pENTR/D-TOPO vectors (Invitrogen) and sequenced. All FBA pENTR clones were then recombined into a diatom adapted pDEST_5′ enhanced yellow fluorescent protein (EYFP) through LR recombination reactions (LR clonase mix, Invitrogen), to generate pEXPR_gene_EYFP vectors driving expression of the genes of interest with an EYFP tag at their C-termini (Siaut et al. 2007). FBA4, the bacteria-like class I FBA, was cloned both with and without a stop codon and recombined into pDEST vectors to generate N- and C-terminal EYFP fusions. The β-CA1 was used as a plastid marker for colocalization with FBA proteins. This gene was PCR amplified from the plasmid pre138-mptca1-enhanced green fluorescent protein (kindly provided by Prof Yusuke Matsuda, Kwansei-Gakuin University, Hyogo, Japan), cloned into a pENTR vector, and recombined into C-terminal cyan fluorescent protein (CFP) fusion pDEST vectors to generate pEXPR_PtCA1_CFP.

Transformation of Wild-Type *P. tricornutum* Cells

The pEXPR plasmids (3 μg) described above were each mixed with pAF6 plasmid (3 μg), which drives expression of the phleomycin-resistance ShBle gene and precipitated onto tungsten microparticles (M-17, Biorad) of 1.1 μm in diameter. The constructs were transfected into *P. tricornutum* wild-type cells by helium-accelerated microparticle bombardment using a BioRad PDS 1000 device following standard procedures described previously (Falciatore et al. 1999). Transformants were selected on solid medium (f/2 with agarose) containing 100 μg/ml phleomycin during 2 weeks, and individual colonies were then transferred to liquid medium for screening for EYFP signal. EYFP positive transformants were maintained in liquid media in the presence of the phleomycin analog xeocin (50 μg/ml); which is lethal for wild-type cells. The EYFP positive transformants have not lost their YFP signal over a period of 3–5 years, and the cultures have maintained resistance indicating long-term stability of transformed constructs.

Epifluorescence Microscopy

Transformant clones were screened for fluorescence 2 days after transfer to antibiotic-containing liquid medium. A Zeiss Axioskop equipped with an HBO 50W UV lamp was used, and the filter 93/XF104-2 (OMEGA), with excitation at 500 nm and emission at 545 nm, was used to detect YFP signal. The filter 93/XF102-2 (excitation 560 nm, emission 595 nm, OMEGA) was also used to acquire chlorophyll autofluorescence images.

Confocal Microscopy

EYFP-positive *P. tricornutum* clones detected by epifluorescence microscopy were observed using a Leica TCS SP2 confocal laser scanning microscope using an HCX PL APO 100x/1.40-0.70 oil objective. EYFP and chlorophyll were excited at 514 nm, CFP was excited at 458 nm, and the resulting fluorescence was filtered using a beam splitter (DD458/514). Fluorescence was detected using a photomultiplier tube with a bandwidth of 525–571 nm for EYFP, 465–551 nm for CFP, and 620–710 nm for chlorophyll autofluorescence. Images were captured with the Leica confocal software and processed with the ImageJ 1.34 software (Wayne Rasband, NIH).

Transmission Electron Microscopy

Three hundred microliters of an FBAC5-EYFP clone batch culture were grown to late exponential phase and harvested by gentle centrifugation. Cells were fixed in 2% glutaraldehyde and embedded in LRWhite medium grade resin (London Resin Company). Ultrathin sections were treated with rabbit anti-GFP antiserum (AbCam) followed by goat anti-rabbit conjugated to electron-dense 10-nm gold particles as described previously (Lichtlé and McKay 1992). Sections were observed with a Jeol CX2 electron microscope at 80 kV.

Quantitative RT-PCR

Cells were cultured in duplicate under Fe replete and deplete conditions, and mRNA was extracted from the four pellets (TRIzol, Invitrogen). RNA concentration was measured by means of an ND-1000 Spectrophotometer (Nanodrop), and SuperScript III reverse polymerase (Invitrogen) was used to convert 100-ng total RNA into cDNA by reverse transcriptase-polymerase chain reaction (RT-PCR). The Fba gene transcripts were quantified by qPCR along with 18S rRNA as an internal control, in triplicate, with each reaction (25 μl) containing 1 μl of the cDNA preparation, 200 nM of forward and reverse primers (supplementary table S2, Supplementary Material online), and 2× SYBR Green I PCR Master Mix (Applied Biosystems, CA). Reactions were run in an Opticon Chromo4 MJ Research Thermal Cycler (Bio-Rad, Hercules, CA). The cycling conditions comprised 10-min polymerase activation at 95 °C and 40 cycles at 95 °C for 15 s and 60 °C for 60 s. The reaction was ended with a 5-min elongation step at 72 °C. Amplicon dissociation (melting) curves were recorded after cycle 40 by heating from 60 to 95 °C with a ramp speed of 0.5 °C every second. The Fba threshold cycles (C_T) were normalized to three endogenous control gene 18S rRNA, TATA binding protein, and H4 (Siaut et al. 2007). Fold difference between Fe replenished and Fe starved cultures measured by means of the $2^{-\Delta\Delta C}$T method (Livak and Schmittgen 2001), where $\Delta\Delta C_T = (C_{T,\ \text{target}} - C_{T,\ 18S})_{5\ \text{nM}} - (C_{T,\ \text{target}} - C_{T,\ 18S})_{1\ \mu\text{M}}$.

FBA Activity Assays

Protein concentrations of cellular extracts were determined by Bradford assay (BioRad, Hercules) according to protocols of the manufacturer. Enzyme activity was measured in an optimized coupled test based on the protocol by Gross et al. (1999). The standard reaction assay contained 100 mM Tricine, pH 7.5; 10 mM $MgCl_2$; 1 U/ml triosephosphate isomerase (TIM); 1 U/ml glycerol-3-phosphate dehydrogenase; NADH (0.2 mM); cellular extract (varying volumes). The decreasing concentration of NADH was monitored spectrophotometrically at $\lambda = 366$ nm. The reaction was started at 25 °C by the addition of 2 mM

fructose-1,6-bisphosphate. Cellular extracts were preincubated in the presence of bivalent ions (10 mM either $MgCl_2$, $MnCl_2$, $ZnCl_2$) or 10 mM EDTA on ice for 1 h. Class II FBAs are dependent on divalent metal ions and are, therefore, inhibited by EDTA (Perham 1990).

Phylogenetic Inference

For each of the diatom FBA genes, the predicted protein model was searched for homologs in a comprehensive genomic database, which we assembled from the nonredundant GenBank CDS database (nr), JGI microbial genomes, and EST libraries (NCBI; ESTdb) for lineages that do not have complete genome data (e.g., red algae and dinoflagellates). Using the iTree phylogenomic pipeline (Moustafa et al. 2010), the homologs for the queries were consolidated at each of the taxonomic ranks (i.e., species, genus, class, order, phylum, and kingdom) to maximize taxon coverage, while maintaining a practical number of taxa. Each query and its homologs were aligned using MAFFT (Katoh et al. 2002; Armbrust et al. 2004; Moustafa et al. 2010) with up to 1,000 refinement iterations. Multiple sequence alignments were manually examined and refined to ensure that key taxa were not missing and to remove ambiguous sites from the alignments. Next, molecular phylogenies were inferred using PhyML (Guindon et al. 2009) with a maximum likelihood and LG amino acid substitution model (Le and Gascuel 2008) and discrete gamma distribution (Yang 1994). Branch confidence values were estimated using the approximate likelihood-ratio test (Anisimova and Gascuel 2006) implementation in PhyML. Only support values greater than 50% were indicated on the graphical representation of the phylogenetic trees. Accession numbers for all sequences analyzed are given in supplementary table S3 (Supplementary Material online).

Results and Discussion

Intracellular Localization and Phylogeny of *P. tricornutum* FBAs

Plastidic FBAs

Observation of multiple positive transformants of C-terminally tagged FBAC1, FBAC2, and FBAC5 confirmed that all three of these proteins are localized in the plastid. The FBAC1-EYFP fusion appears as small spots (usually only one or two) inside the plastid, in a very discrete and precise fashion (fig. 1*A*), with virtually no EYFP background observed elsewhere in the plastid or the cytosol. Although, phylogenetically, FBAC2 seems to be a duplication of FBAC1 (Kroth et al. 2005), its localization was not like FBAC1 but rather appeared to be diffuse throughout the plastid (fig. 1*B*). On the other hand, the class I plastid FBA, FBAC5, typical of higher plants and algae with primary plastids, formed well-defined spots similar to FBAC1-YFP (fig. 1*C*).

To further investigate the subplastidal localization of FBAC1 and FBAC5, *P. tricornutum* β-type CA, PtCA1, which was recently reported to localize to the pyrenoid (Tachibana et al. 2011) was cloned and tagged with a C-terminal CFP fusion, and cotransformed with YFP-tagged FBAC1 and FBAC5. The CA1-CFP signal indeed appeared as punctate spots within the plastid, which colocalized with both FBAC1 and FBAC5 (fig. 2*A* and *B*). It therefore appears that all three proteins localize to the same intraplastidial compartment.

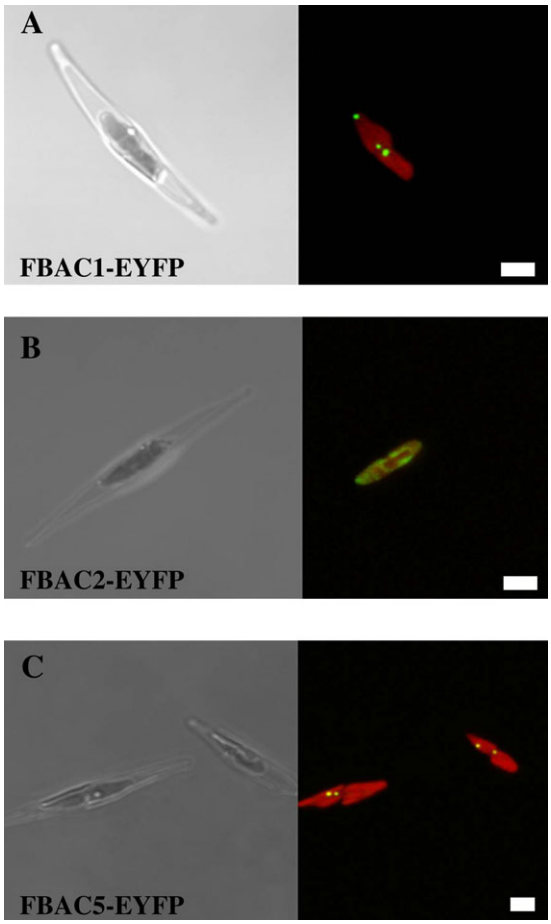

Fig. 1. Localization of plastid FBA-EYFP fusion proteins. (*A*) FBAC1-EYFP, (*B*) FBAC2-EYFP, (*C*) FBAC5-EYFP. On the left light microscopy image, chlorophyll autofluorescence is shown in red and YFP fluorescence in green. Bars, 2 μm.

Immunolocalization of EYFP in transformants expressing FBAC5-EYFP showed clearly that the protein localizes to the pyrenoid (fig. 3). We can conclude that PtCA1, FBAC1, and FBAC5 all localize to pyrenoids within diatom plastids. Pyrenoids are electron-dense bodies known to contain a protein matrix that consists mainly of RuBisCO (Griffiths 1970). Although some classes of microalgae, including certain dinoflagellates, have been reported to activate a CCM in the absence of an observable pyrenoid (Morita et al. 1998; Ratti et al. 2007), the pyrenoid is generally considered to be an important factor for CCM function when present; however, precise function remains unclear (Giordano et al. 2005). Notably, enlargement of pyrenoids has been observed under CO_2 limitation (Izumo et al. 2007), and model simulations of mass spectrometric measurements of cellular carbon fluxes in *P. tricornutum* wild-type and β-CA over expression cells suggested that the pyrenoid is the likely site of CO_2 elevation to concentrations required to saturate

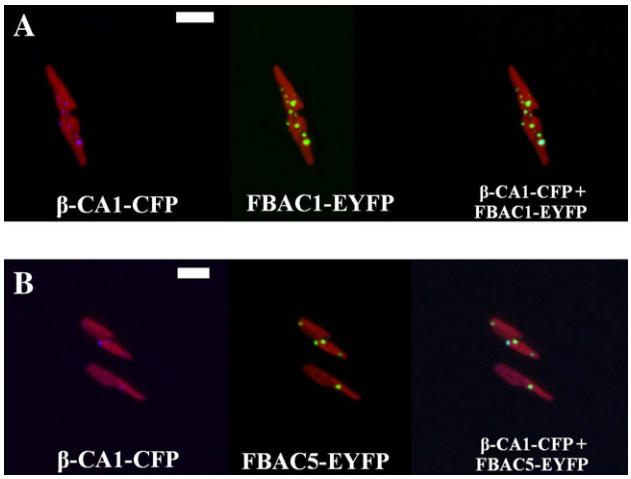

Fig. 2. Colocalization of plastid FBA-YFP with CA1-CFP. (*A*) FBAC1-EYFP + CA1-CFP, (*B*) FBAC5-EYFP + CA1-CFP. Chlorophyll autofluorescence is shown in red, YFP fluorescence in green, and CFP fluorescence in blue. Left image: CFP fluorescence, center: YFP fluorescence, right image: combined fluorescence. Bars, 2 μm.

carbon fixation (Hopkinson et al. 2011). Although the biochemical significance of FBA proteins in the diatom pyrenoid remains to be investigated, it is clear from these experiments that certain members of plastidic class I and II FBA in diatoms have undergone functional diversification related to partitioning some aspects of Calvin cycle activity into the pyrenoid; near the site of CO_2 fixation.

Phylogenetic topology for plastid-localized FBAC5 (fig. 4) suggests a monophyletic relationship among chromalveolate plastids and indicates inheritance from the red algal endosymbiotic ancestor. It is interesting to note that, compared with previous analyses of class I FBA distribution, more thorough taxonomic sampling suggests that cytosolic FBAC5 orthologs are highly diversified and present in most major eukaryotic groups including all the chromalveolates as well as Rhizaria and glaucophytes. Photosynthetic strameonpiles such as the multicellular brown algae *Ectocarpus siliceous* and the pennate diatom *Fragilariopsis cylindrus* also appear to contain cytosolic class I FBA. Curiously, one new well-supported cytosolic clade includes cryptophytes, dinoflagellates, and haptophytes and appears to have originated in these taxa via endosymbiotic gene transfer (EGT).

The plastidic FBAC5 clade is also much expanded relative to previous reports. The most likely explanation for plastidic FBA I (FBAC5) occurrence in the diatom, haptophyte, dinoflagellate algae clade is gene duplication within Archaeplastida prior to the diverge of red algae, followed by EGT from red algae to chromalveolates coupled to selective gene loss within some heterokonts (e.g., centric diatoms). Haptophytes and *Ectocarpus* appear to have a second copy of plastidic FBAC5 that resides in a clade that includes Rhizaria and freshwater green algae.

Class II A FBAs include the plastid-localized copies FBAC1 (pyrenoid) and C2 and cytosolic FBA3. FBAC1 and C2 are members of highly resolved clades comprised of all the major marine phytoplankton taxa including prasinophytes, heterokonts, dinoflagellates, haptophytes, and cryptophytes (fig. 5). The occurrence of prasinophytes within the FBAC2 clade is a new and significant finding and provides some insights into the mystery surrounding the origin of these genes in chromalveolates (Kroth et al. 2005). Considering the well-supported affiliation between prasinophytes and chromalveolates, it seems unlikely that chromalveolate plastid-localized FBAC2 arose by duplication of class II cytosolic FBA3. Rather a more plausible scenario is that, like class I plastid-localized FBAC5, class II plastid FBAC2 was also acquired via EGT. Plastid-targeted nuclear genes of green algal derivation within chromalveolates have been proposed to have arisen from a cryptic endosymbiont related to a prasinophyte-like green alga (Moustafa et al. 2009). An alternative interpretation is that such genes have simply been lost in extant red algae. Regardless of whether the source of the FBA II plastidial EGT event was a green or red algae, it seems apparent that the gene was acquired from a member of the Archaeplastida lineage.

The phylogenetic relationship between prasinophytes and chromalveolates suggests that pyrenoid-associated FBAC1 is the product of an ancient chromalveolate-specific duplication of FbaC2. Due to the occurrence of FBAC1 in each of the four major chromalveolate lineages (heterokonts, alveolates, cryptophytes, and haptophytes), this

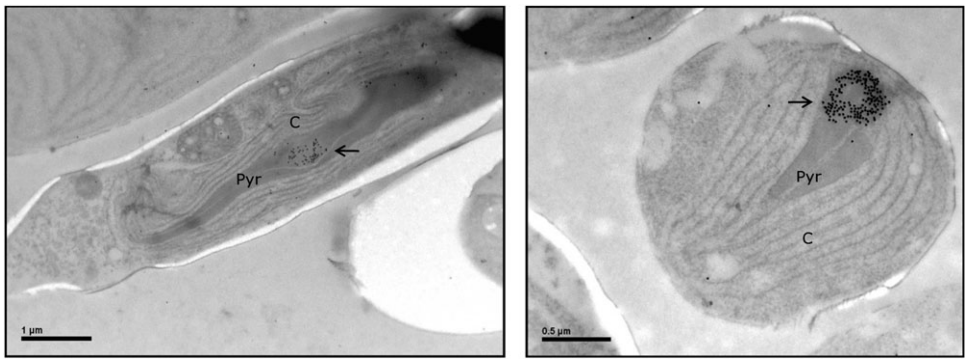

Fig. 3. Localization of *Phaeodactylum tricornutum* FBAC5 by transmission electron microscopy. A clone expressing the FBAC5_EYFP fusions was fixed, and the intracellular EYFP was immunolocalized by means of an anti-GFP antibody. The antibody bound strongly to an intraplastidial structure in FBAC5_EYFP transformant cells. Chloroplasts (C) and pyrenoids (Pyr) and gold particles detected with electron microscopy are indicated. Unlabeled cells did not show any labeling (data not shown).

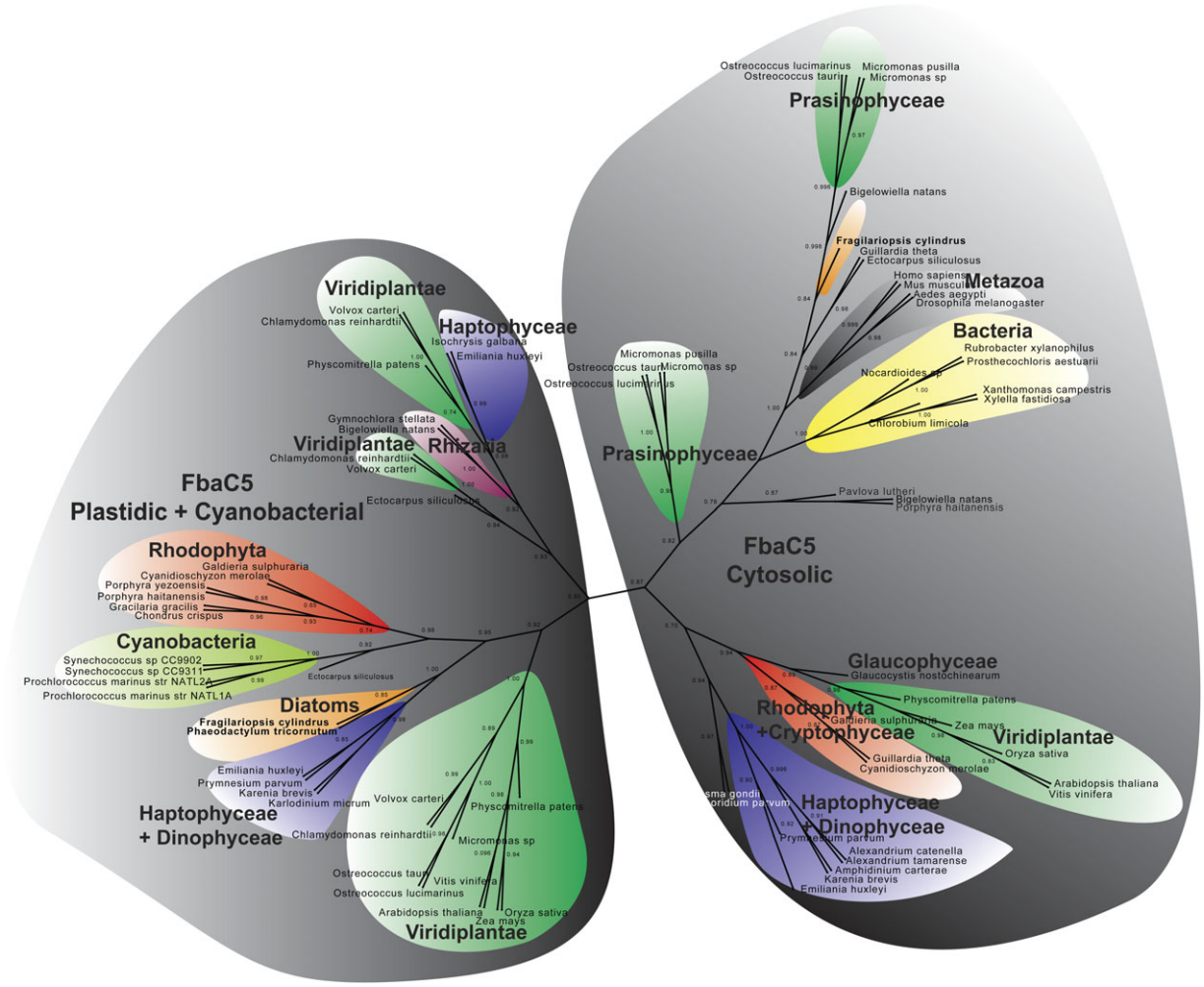

Fig. 4. Protein maximum likelihood phylogeny of class I FBA. Numbers at the nodes indicate approximate likelihood-ratio test support values.

duplication must have occurred prior to chromalveolate diversification. FBAC2, on the other hand, appears to be present only in haptophytes and diatoms and is likely to have been lost within at least some chromalveolates.

Cytosolic FBAs

Cytosolic class II FBA, termed FBA3, displayed a typically cytosolic localization in YFP fusion experiments (fig. 6). Part of the YFP fluorescence appears to concentrate around the plasma membrane or as thin strands within the cell; these regions of dense signal could represent cytosol-rich areas between vacuolar compartments and other organelles (as observed in clones expressing YFP without any targeting signal; data not shown).

The bacterial-class I FBA, called FBA4, showed a similar cytosolic localization both for N-terminal (data not shown) and C-terminal EYFP fusions (fig. 7). In some cells, quite finely defined intracellular lines were observed, much more clearly than in the case of the FBA3. The conspicuous and precisely defined strands surrounding the plastid in the FBA4 transformants may suggests interactions with the cytoskeleton. Interaction of FBA with the cytoskeleton may relate to a role of FBA in motility. In the alveolate *Plasmodium falciparum*, cytosolic FBAs have actin binding activity and play a role in coordinating interactions between cell surface adhesion and cytoskeleton control of parasite motility (Jewett and Sibley 2003).

Prior to diatom genome sequencing, FBA4 had only been described in bacteria. All three diatom genomes sequenced to date contain Fba4, and it was also found in ESTs from the cold-adapted polar diatom *Chaetoceros neogracile* (Jung et al. 2007) (fig. 8). The pelagophyte *Aureococcus* and prasinophyte *Micromonas* also encode genes for FBA4 that form a well-supported clade distinct from diatoms (fig. 8).

Expression and Activity of *P. tricornutum* FBAs

A set of 15 cDNA libraries obtained from mRNA derived from cell cultures grown in different conditions were generated in the context of the *P. tricornutum* genome sequencing project (Bowler et al. 2008; Maheswari et al. 2010). Between 4,000 and 10,000 ESTs were sequenced from each of these cDNA libraries, giving a total collection of around 132,000 sequences that were assembled into about 12,000 transcriptional units (Maheswari et al. 2010). See Maheswari et al. (2010) for a description of culture conditions.

All five FBAs are expressed in several libraries (fig. 9), except for plastid class I FBA, FBAC5, which appears to be

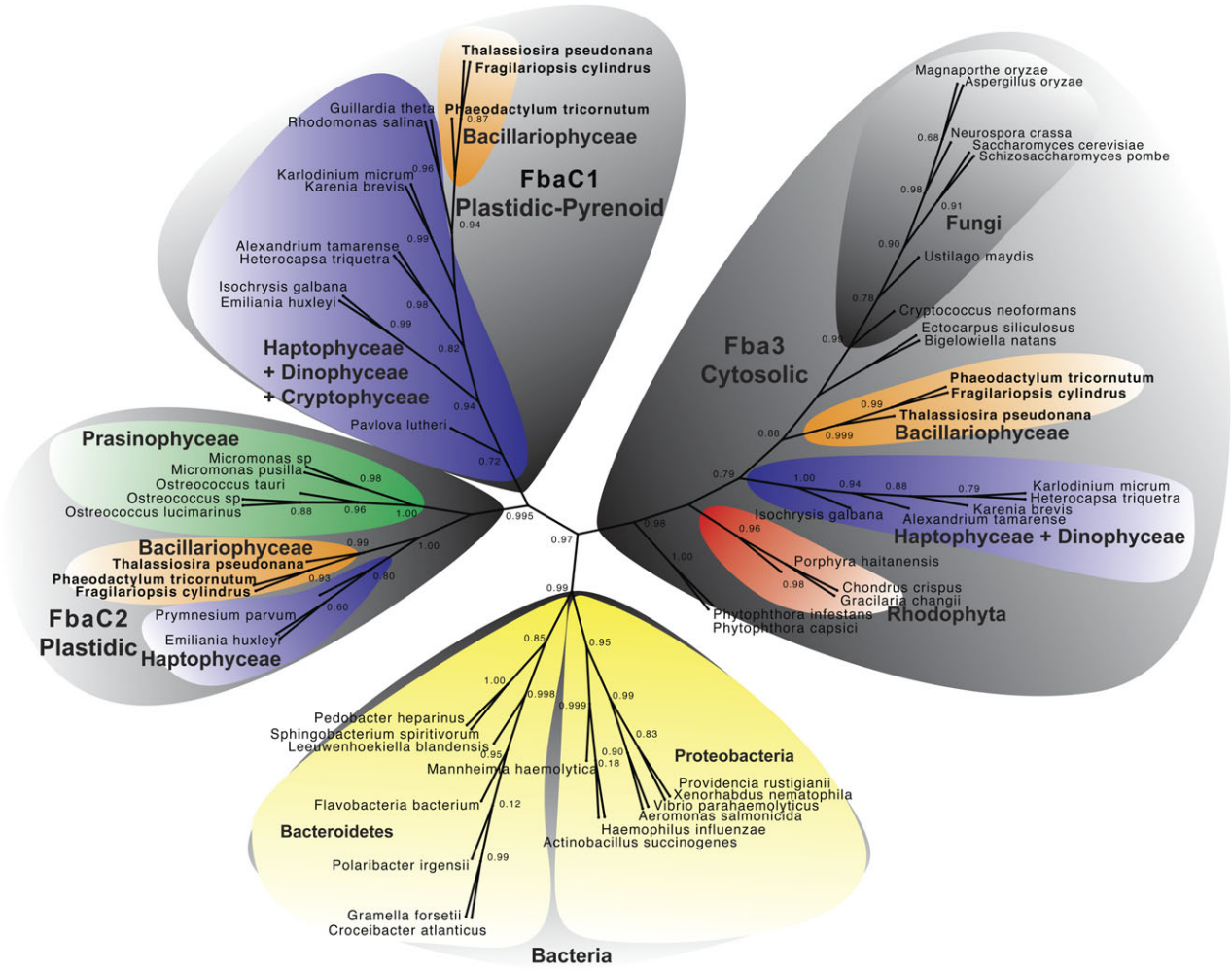

Fig. 5. Protein maximum likelihood phylogeny of class II A FBA. Numbers at the nodes indicate approximate likelihood-ratio test support values.

transcribed only under iron limitation (FL). Similar to FBAC5, plastid class II FBA, *FBAC1*, was also upregulated in Fe limited cultures and additionally in response to blue light (BL). The other plastid class II FBA, *FBAC2*, was also abundant in the blue light library but not under iron limitation. The blue light library was constructed from material harvested after exposure to 2 h of blue light following 48 h in the dark and therefore should represent conditions favorable for C fixation, protein synthesis, and rapid growth.

Cytosolic FBAs also showed an interesting differential expression profile. The class II FBA *FBA3* showed clear upregulation in blue light and to a lesser extent in NO_3^- and Fe limitation. The bacterial-type FBA, *FBA4*, was expressed under a range of different conditions.

The observed EST patterns under Fe limitation were confirmed by quantitative RT-PCR (table 2). It was apparent that plastid class I FBA, *FBAC5*, and plastid class II FBA, *FBAC1*, are upregulated up to 90- and 35-fold, respectively,

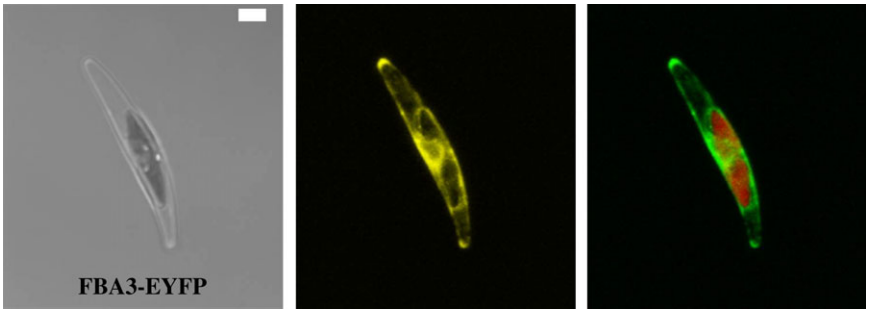

Fig. 6. Localization of FBA3-EYFP fusion proteins. On the left light microscopical image center: YFP fluorescence in yellow and chlorophyll autofluorescence is shown in red. YFP fluorescence is shown in green on the right in order to more easily distinguish the chloroplast. Bars, 2 μm.

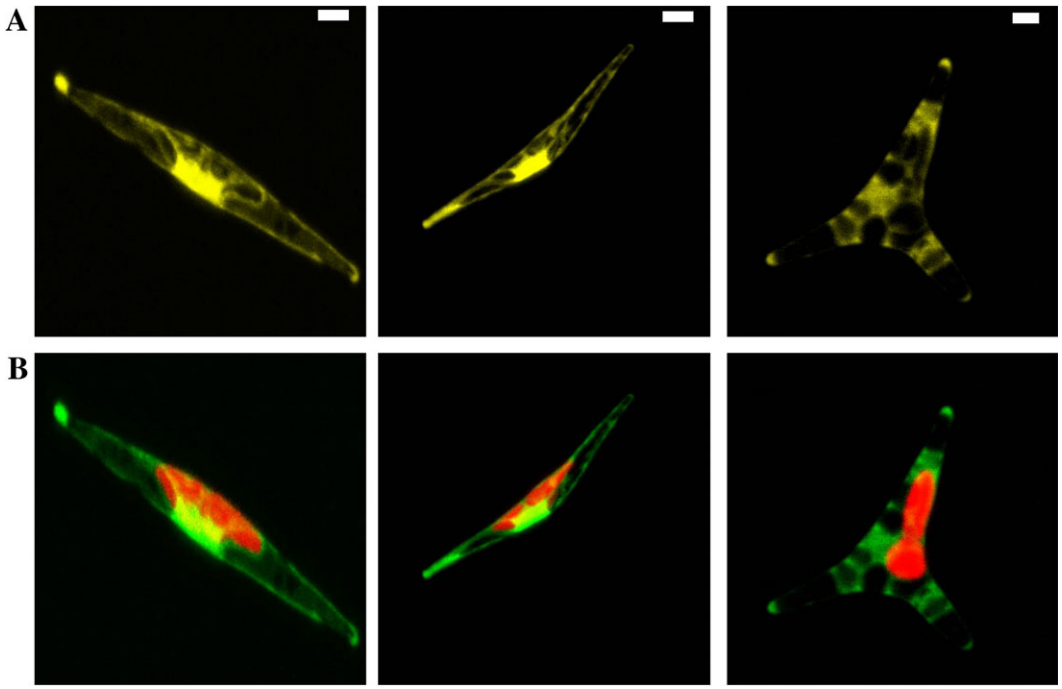

FIG. 7. Localization of FBA4. (*A*) FBA4-EYFP fusion; YFP fluorescence is shown in yellow. (*B*) EYFP-FBA4 fusion; YFP fluorescence is shown in green, chlorophyll autofluorescence in red. Bars, 2 μm.

whereas the other plastid class II FBA, *FBAC2* is strongly downregulated under Fe limitation. The cytosolic class II FBA, *FBA3*, was also found to be more highly expressed under iron limitation (over 10-fold difference), whereas the expression of the bacterial class I *FBA4* is unresponsive to changes in Fe concentration. Furthermore, in experiments using *P. tricornutum* strain Pt4 (UTEX646), we found a clear increase of total FBA and class I FBA activity (measured after inhibition of class II aldolases) compared with cells grown under Fe replete conditions (fig. 10).

Conclusions

FBAs are central to many aspects of cellular C metabolism and are likely relevant for diatom ecophysiological mechanisms of managing acclimation to nutrient limitation and other factors, such as temperature and light availability, that influence C fixation and turnover. Diatoms have a multiplicity of dynamically expressed plastid and cytosolic FBA enzymes likely adapted for management of specific anabolic and catabolic functions in different intracellular compartments under shifting environmental conditions. Preliminary investigation of FBA function in the pennate diatom *P. tricornutum* suggests little functional overlap. The two types of cytosolic FBAs, for example, have very different expression profiles. Diatoms have a class II cytosolic FBA (FBA3), which is a divalent cation-dependent enzyme, as well as a bacterial-like cytosolic class I variant (FBA4) unknown in eukaryotes other than diatoms. The pattern of expression for *FBA3*, encoding a class II cytosolic FBA, suggests a role in both synthesis and mobilization of storage polysaccharides in response to the onset of light and nutrient (Fe and N) limitation conditions, respectively. On the other hand, the expression profile of the bacterial-like *FBA4* indicates a relatively high level of expression in the triradiate morphotype and sensitivity to the presence of silicic acid. Silicate availability greatly influences the distribution and abundance of diatoms in nature, and upregulation in triradiate morphotype cells may be suggestive of a role in cytoskeletal dynamics. Experimental data indicate that *FBA4* expression does not change in response to Fe availability, which combined with the EST data does not suggest a role in central carbon metabolism (e.g., Calvin–Benson cycle and glycolysis). The well-defined cytosolic strands suggestive of cytoskeletal interaction are not as readily observed in FBA3-EYFP. The precise function of diatom-specific FBA4 remains to be uncovered; however, localization and expression data are suggestive of a diatom-specific functional specialization rather than a role in conventional C metabolism.

Whereas the pyrenoid-associated plastid-localized class I FBA, FBAC5, may be upregulated and active specifically under the low Calvin–Benson cycle C flux conditions of Fe limitation, class II pyrenoid-associated FBA (*FBAC1*) was upregulated under Fe limitation as well as in response to the onset of blue light, following a 48-h dark period. By contrast, nonpyrenoid-associated plastid class II FBA (*FBAC2*) was downregulated in response to Fe limitation and stimulated by blue light. Upregulation of *FBAC1* and *FBAC2* gene expression in response to the onset of light suggests a role for these genes under favorable conditions for C fixation.

Confirmation of pyrenoid localization for β-CA in *P. tricornutum* (Tachibana et al. 2011) supports the idea of a biophysical CCM based on transport of HCO_3^- into the plastid followed by conversion of HCO_3^- from the stroma to CO_2 in the pyrenoid near the active site of carbon fixation

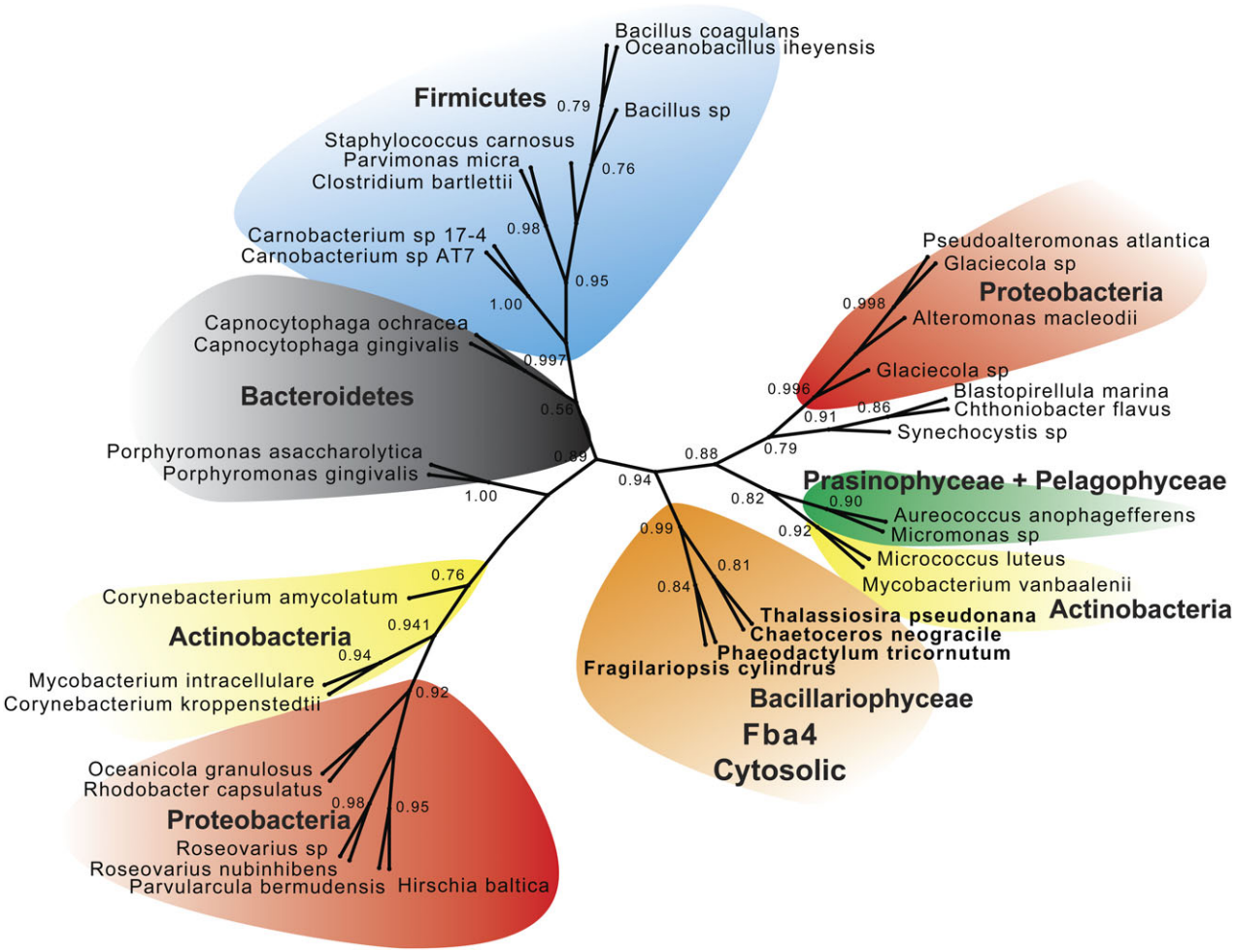

Fig. 8. Protein maximum likelihood phylogeny of class I bacterial-like cytosolic FBA. Numbers at the nodes indicate approximate likelihood-ratio test support values.

(Hopkinson et al. 2011), as previously hypothesized (Roberts et al. 2007a, 2007b). The occurrence of class I and II FBAs, FBAC5 and FBAC1, in the pyrenoid of *P. tricornutum* might implicate linkage between some components of the Calvin–Benson cycle and the CCM. FBAs catalyze the first step in the regeneration of the 5 carbon (C) ribulose compound that is the substrate for RuBisCO, CO_2 fixation, and generation of new C_3 sugars. It is possible, therefore, that the FBA catalyzed conversion of C_3 to C_6 molecules serves to partially regulate CO_2 fluxes into the Calvin–Benson cycle. In the vascular plant *Arabidopsis thaliana*, FBA is 1 of 3 Calvin cycle enzymes, along with RuBisCO and SBPAse, that was most sensitive to biological perturbations and found to have an important rate-limiting role in regulating the carbon assimilation flux of the Calvin cycle (Haake et al. 1998; Sun et al. 2003).

In photosynthetically active plastids, FBA activity is necessary for regeneration of Ru 1,5-BP and should therefore operate principally in the direction of Fru1,6-BP formation, as suggested by antisense inhibition of FBA in potato plants (Haake et al. 1998). Under optimal conditions for C fixation, prior to generation of C_5 RuBisCO substrate, C_6 compounds, generated from FBA activity, prime the regeneration phase of the Calvin–Benson cycle, and subsequently for every C_6 molecule that is used, 5 of 6 are recycled and 1 of 6 constitutes net gain. However, in situations in which inorganic C fixation is constrained, the reverse reaction (Zgiby et al. 2000) may occur to permit sufficient flow of C through the triose pool for respiration and biosynthesis of other C molecules. Indeed, gene expression, metabolite, and physiological data indicate an overall retrenchment of C fixation in response to Fe limitation, a condition which has been globally assayed in detail in *P. tricornutum* (Allen et al. 2008), including downregulation for genes encoding β-CA, phosphoribulokinase (PRK), and fructose 1,6-bisphosphatase (FBPase) (Allen et al. 2008), all of which would be coherent with reduction of C_5 regeneration. Consistent with the idea of FBA-mediated production and associated chloroplast export of trioses, plastid triose isomerases and plastid-envelope triose/hexose phosphate translocators are upregulated under Fe limitation (Allen et al. 2008).

In some microalgae, storage polysaccharides have been shown to be mobilized in nitrogen (N), C, Fe, and light-limited cultures (Varum and Myklestad 1984; Granum and Myklestad 2001; Allen et al. 2008), and in addition to

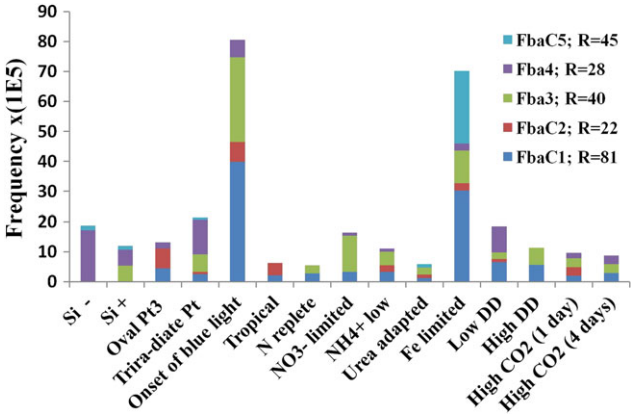

FIG. 9. Expression of *Phaeodactylum tricornutum FBA* genes according to their normalized frequency of observation in a range of cDNA libraries representing different environmental conditions (Maheswari et al. 2010). Normalized expression values were obtained by dividing the number of *FBA* ESTs in the different libraries by the total number of sequences generated for the different libraries. The *R* value was defined in Stekel et al. (2000), an *R* value above 12 indicates nonspurious differences in the EST frequency across libraries (i.e., differential expression). The features of the 15 libraries have been published elsewhere (Allen et al. 2008; Sapriel et al. 2009; Maheswari et al. 2010). Si− = f/2 with artificial seawater, no Si added; Si+ = 350 μM metasilicate; Oval = Oval strain CCAP1052/1B; Triradiate = Triradiate strain NEPCC640; Blue light = Cells grown in the dark for 48 h and subjected to blue light for 1 h; Tropical = Tropical strain CCMP633 grown at a suboptimal temperature of 18 °C; N replete = 1.12 mM chemostat culture; NO3 starved = 50 μM in chemostat culture for 12 days; Urea adapted = 50 μM Urea; Fe deplete = 5 nM Iron; Low DD = 0.5 μg/ml 2E,4E-decadienal for 6 h; High DD = 5 μg/ml 2E,4E-decadienal for 6 h (for a full description of culture conditions, see Maheswari et al. 2010).

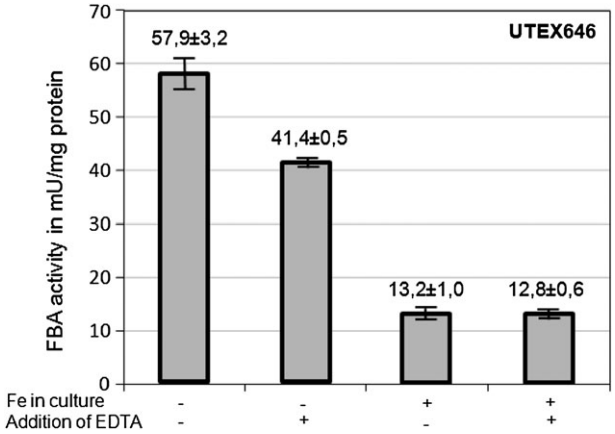

FIG. 10. FBA activity in *Phaeodactylum tricornutum* (UTEX646) cells grown for 5 days in Fe deplete and replete medium. Enzymatic activity is given as mU/mg total cellular soluble protein. The measurements were performed in either presence or absence of EDTA to measure class I FBA activity or total FBA activity, respectively.

supplying respiratory substrate, may be imported into the plastid to ensure the continued biosynthesis of essential metabolites (such as fatty acids) under impaired C fixation conditions. Consequently, a possible upregulation of genes encoding FBAC1 and FBAC5 could imply a role in the maintenance of carbon flow through C_3 and C_4 pools for the synthesis of lipids, nucleotides, and other metabolites. Given that diatoms do not have an oxidative pentose phosphate pathway in their plastids (Michels et al. 2005) and neither do they have storage polysaccharides within them, the mobilization of C_3 or C_6 molecules across plastid membranes during impaired C fixation could be necessary for the continued supply of C building blocks for anabolic processes. In contrast, the expression profile of cytosolic class II FBA, FBA 3, which is upregulated under N and Fe limitation and in response to the onset of blue light, is consistent with a role in catabolic C flow through glycolysis.

Most algal genomes encode between 2 and 3 plastid localized FBAs and 1 or 2 cytosolic copies. In diatoms, class II cytosolic FBA, FBA3, appears to be the only FBA that is likely to have originated with the secondary endosymbiotic host nucleus; the other four diatom FBAs appear to have originated from lateral transfer from bacteria and from plastid acquisition. In contrast to plants and freshwater algae, all the major marine unicellular eukaryotic phytoplankton lineages, prasinophytes, haptophytes, dinoflagellates, diatoms, and cryptophytes, encode plastid-targeted copies of class I and II FBA. Chromalveolate taxa are distinguished by a second copy of class II plastid FBA, FBAC1, which, in *P. tricornutum*, appears to function in the pyrenoid region of the plastid. The most parsimonious explanation for the origin of FBAC1 is a chromalveolate-specific duplication of FBAC2, which appears to have originated by EGT from green algae. The overall pattern of FBA diversity within and between chromalveolates could be interpreted with the context of either the chromalveolate or serial hypothesis for the origin of plastids in chromalveolates (Baurain et al. 2010). In the latter scenario, FBAC2 duplication would have occurred in the founder alga that subsequently engaged in eukaryote–eukaryote endosymbiosis with various hosts. The presence of FBAC2 in diatoms and haptophytes perhaps suggests shared host ancestry at the time of FBA2 acquisition—via EGT from a cryptic green algal endosymbiont. The idea that chromalveolates have recruited genes separately from red and green algae (Moustafa et al. 2009) seems to be typified by plastid-localized FBAs whereby one copy, class I FBA (FBAC5), appears to have originated from red algal EGT and the other two copies, class II FBAs (FBAC1 and FBAC2), seem to have been acquired via EGT from a prasinophyte-like green alga followed by a chromalveolate-specific duplication.

Table 2. Fold Variation of FBA Gene Expression Observed in Fe-Limited Cultures with Respect to Fe Replete Cultures (5 nM vs. 10 μM).

	Experiment 1	Experiment 2
FbaC1	26.1 ± 2.2	45.3 ± 5.2
FbaC2	−22.9 ± 0.7	−36.0 ± 33.5
Fba3	13.0 ± 3.1	16.7 ± 2.9
Fba4	1.2 ± 0.2	1.4 ± 0.2
FbaC5	86.4 ± 23.9	100.8 ± 28.0

NOTE.—Two identical experiments were conducted on different dates; the fold change was calculated by the $2^{-\Delta\Delta\ C}T$ method (see Materials and Methods). The values shown are averages and standard deviations of two replicate mRNA extractions.

Supplementary Material

Supplementary tables S1–S3 are available at *Molecular Biology and Evolution* online (http://www.mbe.oxfordjournals.org/).

Acknowledgments

We would like to thank Agnès Meichenin and Christiane Lichtlé for assistance with electron microscopy analysis and Yusuke Matsuda for providing the PtCA1 gene. This work was supported by grants from the Agence Nationale de la Recherche and the European Commission awarded to C.B., from the National Science Foundation awarded to A.E.A. (NSF OCE 0727997 and NSF OCE 0722374) and a grant from the German Research Foundation (DFG) (KR 1661/4-1) to P.G.K., and by the University of Konstanz.

References

Allen AE, Dupont CL, Obornik M, et al. (11 co-authors). 2011. Evolution and metabolic significance of the urea cycle in photosynthetic diatoms. *Nature* 473:203–207.

Allen AE, LaRoche J, Maheswari U, Lommer M, Schauer N, Lopez PJ, Finazzi G, Fernie AR, Bowler C. 2008. Whole-cell response of the pennate diatom Phaeodactylum tricornutum to iron starvation. *Proc Natl Acad Sci U S A.* 105:10438–10443.

Allen AE, Vardi A, Bowler C. 2006. An ecological and evolutionary context for integrated nitrogen metabolism and related signaling pathways in marine diatoms. *Cur Opin Plant Biol.* 9:264–273.

Anisimova M, Gascuel O. 2006. Approximate likelihood-ratio test for branches: a fast, accurate, and powerful alternative. *Syst Biol.* 55:539–552.

Anita N. 1967. Comparative studies on aldolase activity in marine planktonic algae and their evolutionary significance. *J Phycol.* 3:81–85.

Armbrust EV. 2009. The life of diatoms in the world's oceans. *Nature* 459:185–192.

Armbrust EV, Berges JA, Bowler C, et al. (45 co-authors). 2004. The genome of the diatom Thalassiosira pseudonana: ecology, evolution, and metabolism. *Science* 306:79–86.

Badger MR, Andrews TJ, Whitney SM, Ludwig M, Yellowlees DC, Leggat W, Price GD. 1998. The diversity and coevolution of Rubisco, plastids, pyrenoids, and chloroplast-based CO2-concentrating mechanisms in algae. *Canadian J Botany-Revue Canadienne De Botanique.* 76:1052–1071.

Baurain D, Brinkmann H, Petersen J, Rodriguez-Ezpeleta N, Stechmann A, Demoulin V, Roger AJ, Burger G, Lang BF, Philippe H. 2010. Phylogenomic evidence for separate acquisition of plastids in cryptophytes, haptophytes, and stramenopiles. *Mol Biol Evol.* 27:1698–1709.

Behrenfeld MJ, Bale AJ, Kolber ZS, Aiken J, Falkowski PG. 1996. Confirmation of iron limitation of phytoplankton photosynthesis in the equatorial Pacific Ocean. *Nature* 383:508–511.

Behrenfeld MJ, Worthington K, Sherrell RM, Chavez FP, Strutton P, McPhaden M, Shea DM. 2006. Controls on tropical Pacific Ocean productivity revealed through nutrient stress diagnostics. *Nature* 442:1025–1028.

Bowler C, Allen AE, Badger JH, et al. (76 co-authors). 2008. The Phaeodactylum genome reveals the evolutionary history of diatom genomes. *Nature* 456:239–244.

Bowler C, Vardi A, Allen AE. 2010. Oceanographic and biogeochemical insights from diatom genomes. *Ann Rev Mar Sci.* 2:333–365.

Cavalier-Smith T. 2000. Membrane heredity and early chloroplast evolution. *Trends Plant Sci.* 5:174–182.

Falciatore A, Casotti R, Leblanc C, Abrescia C, Bowler C. 1999. Transformation of nonselectable reporter genes in marine diatoms. *Mar Biotechnol.* 1:239–251.

Field CB, Behrenfeld MJ, Randerson JT, Falkowski P. 1998. Primary production of the biosphere: integrating terrestrial and oceanic components. *Science* 281:237–240.

Flechner A, Gross W, Martin WF, Schnarrenberger C. 1999. Chloroplast class I and class II aldolases are bifunctional for fructose-1,6-biphosphate and sedoheptulose-1,7-biphosphate cleavage in the Calvin cycle. *Febs Lett.* 447:200–202.

Giordano M, Beardall J, Raven JA. 2005. CO2 concentrating mechanisms in algae: mechanisms, environmental modulation, and evolution. *Annu Rev Plant Biol.* 56:99–131.

Granum E, Myklestad S. 2001. Mobilization of ß-1,3-glucan and biosynthesis of amino acids induced by NH4+ addition to N-limited cells of the marine diatom Skeletonema costatum. *J Phycol.* 37:772–782.

Granum E, Raven JA, Leegood RC. 2005. How do marine diatoms fix 10 billion tonnes of inorganic carbon per year? *Canadian J Botany-Revue Canadienne De Botanique.* 83:898–908.

Griffiths DJ. 1970. The pyrenoid. *Botanical Rev.* 36:29–58.

Gross W, Bayer MG, Schnarrenberger C, Gebhart G, Maier TL, Schenk H. 1994. Two distinct aldolases of class II type in the cyanoplasts and in the cytosol of the alga Cyanophora paradoxa. *Plant Physiol.* 105:1393–1398.

Gross W, Lenze D, Nowitzki U, Weiske J, Schnarrenberger C. 1999. Characterization, cloning, and evolutionary history of the chloroplast and cytosolic class I aldolases of the red alga Galdieria sulphuraria. *Gene* 230:7–14.

Guillard RRL. 1975. Culture of phytoplankton for feeding marine invertebrates. In: Smith WL, Chanley MH, editors. Culture of marine invertebrate animals. New York: Plenum Press. p. 26–60.

Guindon S, Delsuc F, Dufayard JF, Gascuel O. 2009. Estimating maximum likelihood phylogenies with PhyML. *Methods Mol Biol.* 537:113–137.

Haake V, Zrenner R, Sonnewald U, Stitt M. 1998. A moderate decrease of plastid aldolase activity inhibits photosynthesis, alters the levels of sugars and starch, and inhibits growth of potato plants. *Plant J.* 14:147–157.

Hopkinson BM, Dupont CL, Allen AE, Morel FM. 2011. Efficiency of the CO2-concentrating mechanism of diatoms. *Proc Natl Acad Sci U S A.* 108:3830–3837.

Izumo A, Fujiwara S, Oyama Y, Satoh A, Fujita N, Nakamura Y, Tsuzuki M. 2007. Physicochemical properties of starch in Chlorella change depending on the CO2 concentration during growth: comparison of structure and properties of pyrenoid and stroma starch. *Plant Sci.* 172:1138–1147.

Jacobshagen S, Schnarrenberger C. 1990. Two class I aldolases in Klebsormidium flaccidum (CHAROPHYCEAE): an evolutionary link from chlorophytes to higher plants. *J Phycol.* 26:312–317.

Janouskovec J, Horak A, Obornik M, Lukes J, Keeling PJ. 2010. A common red algal origin of the apicomplexan, dinoflagellate, and heterokont plastids. *Proc Natl Acad Sci U S A.* 107: 10949–10954.

Jewett TJ, Sibley LD. 2003. Aldolase forms a bridge between cell surface adhesins and the actin cytoskeleton in apicomplexan parasites. *Mol Cell.* 11:885–894.

Jung G, Lee CG, Kang SH, Jin E. 2007. Annotation and expression profile analysis of cDNAs from the Antarctic diatom Chaetoceros neogracile. *J Microbiol Biotechnol.* 17:1330–1337.

Kaplan A, Reinhold L. 1999. CO2 concentrating mechanisms in photosynthetic microorganisms. *Annu Rev Plant Physiol Plant Molec Biol.* 50:539–570.

Katoh K, Misawa K, Kuma K, Miyata T. 2002. MAFFT: a novel method for rapid multiple sequence alignment based on fast Fourier transform. *Nucleic Acids Res.* 30:3059–3066.

Kitao Y, Harada H, Matsuda Y. 2008. Localization and targeting mechanisms of two chloroplastic β-carbonic anhydrases in the marine diatom Phaeodactylum tricornutum. *Physiol Plant.* 133:68–77.

Kroth PG, Chiovitti A, Gruber A, et al. 2008. A model for carbohydrate metabolism in the diatom *Phaeodactylum tricornutum* deduced from comparative whole genome analysis. *PLoS One* 3:e1426.

Kroth PG, Schroers Y, Kilian O. 2005. The peculiar distribution of class I and class II aldolases in diatoms and in red algae. *Curr Genet.* 48:389–400.

Kustka A, Allen AE, Morel FMM. 2007. Sequence analysis and transcriptional regulation of Fe acquisition genes in two marine diatoms. *J Phycol.* 43:715–729.

Le SQ, Gascuel O. 2008. An improved general amino acid replacement matrix. *Mol Biol Evol.* 25:1307–1320.

Lichtlé C, McKay RML. 1992. Immunogold localization of photosystem I and photosystem II light-harvesting complexes in cryptomonad thylakoids. *Biol Cell.* 72:187–194.

Livak KJ, Schmittgen TD. 2001. Analysis of relative gene expression data using real-time quantitative PCR and the 22DDCT method. *Methods* 25:402–408.

Maheswari U, Jabbari K, Petit J, et al. (20 co-authors). 2010. Digital expression profiling of novel diatom transcripts provides insight into their biological functions. *Genome Biol.* 11:R85.

Marsh JJ, Lebherz HG. 1992. Fructose-bisphosphate aldolases—an evolutionary history. *Trends Biochem Sci.* 17:110–113.

McGinn PJ, Morel FMM. 2008. Expression and inhibition of the carboxylating and decarboxylating enzymes in the photosynthetic C-4 pathway of marine diatoms. *Plant Physiol.* 146:300–309.

Michels AK, Wedel N, Kroth PG. 2005. Diatom plastids possess a phosphoribulokinase with an altered regulation and no oxidative pentose phosphate pathway. *Plant Physiol.* 137:911–920.

Milligan AJ, Harrison PJ. 2000. Effects of non-steady-state iron limitation on nitrogen assimilatory enzymes in the marine diatom Thalassiosira weissflogii (Bacillariophyceae). *J Phycol.* 36:78–86.

Montsant A, Jabbari K, Maheswari U, Bowler C. 2005. Comparative genomics of the pennate diatom Phaeodactylum tricornutum. *Plant Physiol.* 137:500–513.

Morita E, Abe T, Tsuzuki M, Fujiwara S, Sato N, Hirata A, Sonoike K, Nozaki H. 1998. Presence of the CO2-concentrating mechanism in some species of the pyrenoid-less free-living algal genus Chloromonas (Volvocales, Chlorophyta). *Anglais* 204:269–276.

Moustafa A, Beszteri B, Maier UG, Bowler C, Valentin K, Bhattacharya D. 2009. Genomic footprints of a cryptic plastid endosymbiosis in diatoms. *Science* 324:1724–1726.

Moustafa A, Bhattacharya D, Allen AE. 2010. iTree: a high-throughput phylogenomic pipeline. Proceedings of the 2010 5th Cairo International Biomedical Engineering Conference (CIBEC); 2010 Dec 16–18; Cairo, Egypt. New York (NY): Institute of Electrical and Electronics Engineers.

Parker MS, Mock T, Armbrust EV. 2008. Genomic insights into marine microalgae. *Annu Rev Genet.* 42:619–645.

Patron NJ, Rogers MB, Keeling PJ. 2004. Gene replacement of fructose-1,6-bisphosphate aldolase supports the hypothesis of a single photosynthetic ancestor of chromalveolates. *Eukaryot Cell.* 3:1169–1175.

Pelzer-Reith B, Penger A, Schnarrenberger C. 1993. Plant aldolase: cDNA and deduced amino-acid sequences of the chloroplast and cytosol enzyme from spinach. *Plant Mol Biol.* 21:331–340.

Perham RN. 1990. The Fructose-1,6-bisphosphate aldolases—same reaction, different enzymes. *Biochem Soc Trans.* 18:185–187.

Ratti S, Giordano M, Morse D. 2007. CO2-concentrating mechanisms of the potentially toxic dinoflagellate Protoceratium reticulatum (Dinophyceae, Gonyaulacales). *J Phycol.* 43:693–701.

Reinfelder JR. 2011. Carbon concentrating mechanisms in eukaryotic marine phytoplankton. Annual Review of Marine Science, Vol 3. Palo Alto (CA): Annual Reviews. p. 291–315.

Reinfelder JR, Kraepiel AML, Morel FMM. 2000. Unicellular C-4 photosynthesis in a marine diatom. *Nature* 407:996–999.

Reinfelder JR, Milligan AJ, Morel FMM. 2004. The role of the C-4 pathway in carbon accumulation and fixation in a marine diatom. *Plant Physiol.* 135:2106–2111.

Riebesell U, Wolfgladrow DA, Smetacek V. 1993. Carbon-dioxide limitation of marine-phytoplankton growth-rates. *Nature* 361:249–251.

Roberts K, Granum E, Leegood RC, Raven JA. 2007a. C-3 and C-4 pathways of photosynthetic carbon assimilation in marine diatoms are under genetic, not environmental, control. *Plant Physiol.* 145:230–235.

Roberts K, Granum E, Leegood RC, Raven JA. 2007b. Carbon acquisition by diatoms. *Photosynth Res.* 93:79–88.

Rogers M, Keeling PJ. 2004. Lateral transfer and recompartmentalization of Calvin cycle enzymes of plants and algae. *J Mol Evol.* 58:367–375.

Round FE, Crawford RW, Mann DG. 1990. The Diatoms. Biology and Morphology of the Genera. New York: Cambridge University Press.

Sanchez LB, Horner DS, Moore DV, Henze K, Embley TM, Muller M. 2002. Fructose-1,6-bisphosphate aldolases in amitochondriate protists constitute a single protein subfamily with eubacterial relationships. *Gene* 295:51–59.

Sapriel G, Quinet M, Heijde M, Jourdren L, Tanty V, Luo G, Le Crom S, Lopez PJ. 2009. Genome-wide transcriptome analyses of silicon metabolism in *Phaeodactylum tricornutum* reveal the multilevel regulation of silicic acid transporters. *PLoS One.* 4:e7458.

Siaut M, Heijde M, Mangogna M, Montsant A, Coesel S, Allen A, Manfredonia A, Falciatore A, Bowler C. 2007. Molecular toolbox for studying diatom biology in Phaeodactylum tricornutum. *Gene* 406:23–35.

Stekel DJ, Git Y, Falciani F. 2000. The comparison of gene expression from multiple cDNA libraries. *Genome Res.* 10:2055–2061.

Sun N, Ma LG, Pan DY, Zhao HY, Deng XW. 2003. Evaluation of light regulatory potential of Calvin cycle steps based on large-scale gene expression profiling data. *Plant Mol Biol.* 53: 467–478.

Sunda W, Huntsman S. 2003. Effect of pH, light, and temperature on Fe-EDTA chelation and Fe hydrolysis in seawater. *Mar Chem.* 84:35–47.

Tachibana M, Allen A, Kikutani S, Endo Y, Bowler C, Matsuda Y. Localization of putative carbonic anhydrases in two marine diatoms, Phaeodactylum tricornutum and Thalassiosira pseudonana. *Photosynth Res.* Advance Access published March 2, 2011, doi:10.1007/s11120-011-9634-4.

Tanaka Y, Nakatsuma D, Harada H, Ishida M, Matsuda Y. 2005. Localization of soluble beta-carbonic anhydrase in the marine diatom Phaeodactylum tricornutum. Sorting to the chloroplast and cluster formation on the girdle lamellae. *Plant Physiol.* 138:207–217.

Varum KM, Myklestad S. 1984. Effects of light, salinity and nutrient limitation on the production of -1,3-D-Glucan and Exo-D-Glucanase activity in Skeletonema costatum. *J Exp Mar Biol Ecol.* 83:13–26.

Wilhelm C, Buchel C, Fisahn J, et al. (12 co-authors). 2006. The regulation of carbon and nutrient assimilation in diatoms is significantly different from green algae. *Protist* 157:91–124.

Yang Z. 1994. Maximum likelihood phylogenetic estimation from DNA sequences with variable rates over sites: approximate methods. *J Mol Evol.* 39:306–314.

Yoon HS, Hackett JD, Pinto G, Bhattacharya D. 2002. The single, ancient origin of chromist plastids. *Proc Natl Acad Sci U S A.* 99:15507–15512.

Zgiby SM, Thomson GJ, Qamar S, Berry A. 2000. Exploring substrate binding and discrimination in fructose1,6-bisphosphate and tagatose 1,6-bisphosphate aldolases. *Eur J Biochem.* 267:1858–1868.